THE JOURNAL OF BIOLOGICAL CHEMISTRY VOL. 287, NO. 28, pp. 23271–23282, July 6, 2012

Nigericin-induced Impairment of Autophagic Flux in Neuronal Cells Is Inhibited by Overexpression of Bak*[S]

Received for publication, March 21, 2012, and in revised form, April 4, 2012 Published, JBC Papers in Press, April 5, 2012, DOI 10.1074/jbc.M112.364281

Junghyun Lim[‡], Yunsu Lee[‡], Hyun-Wook Kim[§], Im Joo Rhyu[§], Myung Sook Oh[¶], Moussa B. H. Youdim[‖], Zhenyu Yue[**], and Young J. Oh[‡1]

*From the [‡]Department of Biology, Yonsei University College of Life Science and Biotechnology, 134 Shinchon-dong Seodaemoon-gu, Seoul 120-749, Korea, the [§]Department of Anatomy, College of Medicine, Korea University, Seoul 136-705, Korea, the [¶]Department of Life and Nanopharmaceutical Science, Kyung Hee University, Seoul 130-701, Korea, [‖]Technion Israel Institute of Technology, Haifa 31096, Israel, and the **Department of Neurology and Neuroscience, Friedman Brain Institute, Mount Sinai School of Medicine, New York, New York 10029*

Background: Exact mechanisms underlying regulatory roles for the Bcl-2 family remain to be delineated.
Results: Overexpressed Bak blocked ionophore-induced impairment of autophagic flux in neuronal cells.
Conclusion: Bak plays critical roles in maintaining autophagic flux and vacuole homeostasis.
Significance: Our findings contribute to better understanding of the Bcl-2 family's potential as a novel therapeutic strategy in autophagy-associated neurodegeneration.

Bak is a prototypic pro-apoptotic Bcl-2 family protein expressed in a wide variety of tissues and cells. Recent studies have revealed that Bcl-2 family proteins regulate apoptosis as well as autophagy. To investigate whether and how Bak exerts a regulatory role on autophagy-related events, we treated independent cell lines, including MN9D neuronal cells, with nigericin, a K^+/H^+ ionophore. Treatment of MN9D cells with nigericin led to an increase of LC3-II and p62 levels with concomitant activation of caspase. Ultrastructural examination revealed accumulation of autophagic vacuoles and swollen vacuoles in nigericin-treated cells. We further found that the LC3-II accumulated as a consequence of impaired autophagic flux and the disrupted degradation of LC3-II in nigericin-treated cells. In this cell death paradigm, both transient and stable overexpression of various forms of Bak exerted a protective role, whereas it did not inhibit the extent of nigericin-mediated activation of caspase-3. Subsequent biochemical and electron microscopic studies revealed that overexpressed Bak maintained autophagic flux and reduced the area occupied by swollen vacuoles in nigericin-treated cells. Similar results were obtained in nigericin-treated non-neuronal cells and another proton ionophore-induced cell death paradigm. Taken together, our study indicates that a protective role for Bak during ionophore-induced cell death may be closely associated with its regulatory effect on maintenance of autophagic flux and vacuole homeostasis.

Autophagy is an evolutionarily conserved catabolic process involved in cellular homeostasis and stress responses, including the degradation of target proteins or organelles through lysosomal pathways (1). Among the three types of autophagy (*e.g.* macroautophagy, microautophagy, and chaperone-mediated autophagy), macroautophagy encompasses the formation of autophagosome and the subsequent autolysosome after fusion with the lysosome (2). Among several molecules involved in autophagy, LC3 has been widely used as a marker of autophagy. Because soluble cytosolic LC3-I is modified through lipidation and predominantly associated with the autophagosomal membrane, the levels of LC3-II that form in a given situation can be used to predict the extent of autophagosome formation (3). As the LC3-II is degraded after fusion between autophagosomes and lysosomes, increased levels of LC3-II can result from either induced synthesis of autophagosomes or a reduced rate of degradation (4). Maturation of autophagosomes is a multistep process involving fusion with early or late endosomes, such as multivesicular bodies (MVBs),[2] yielding the amphisome, prior to fusion with lysosomes (5, 6). Any defects in this process can impair autophagic flux, leading to the accumulation of LC3-II. Functional MVBs or endosomal compartments are required for efficient autophagosomal maturation. In some pathological conditions, it has been reported that impaired MVBs or endosomal proteins lead to abnormal autophagic degradation (7–9).

Cell death modality has been routinely classified as apoptosis, necrosis, or autophagic cell death (10). Although there have been debates as to whether autophagy *per se* executes cell death or whether it represents a cytoprotective process (11, 12), there is a growing body of evidence supporting the involvement of *bona fide* autophagic cell death in various forms of pathophysiological situations (13). Intriguingly, these distinct forms of cell death do not seem to occur in a mutually exclusive way, but rather cell death can be accompanied by mixed features of multiple cell death mechanisms at the same time or sequentially (14, 15). Furthermore, the interrelationship between autophagy

* This work was supported by grants from the Ministry of Science and Technology through BRC, and in part by the Korea Science and Engineering Foundation (SRC, 2012-0000496) and the Mid-Career Research Program through NRF funded by the Ministry of Education, Science, and Technology (to Y. J. O.).
[S] This article contains supplemental Figs. S1–S4.
[1] To whom correspondence should be addressed. Tel.: 82-2-2123-2662; Fax: 82-2-312-5657; E-mail: yjoh@yonsei.ac.kr.

[2] The abbreviations used are: MVB, multivesicular body; MEF, mouse embryo fibroblast; Z, benzyloxycarbonyl; AV, autophagic vacuole; MTT, 3-(4,5-dimethylthiazol-2-yl)-2,5-diphenyltetrazolium bromide; BH3 domain, Bcl-2 homology domain 3.

and apoptosis has recently attracted much attention (13, 15). These two distinct cell death modalities can act in a cooperative manner to invoke cell death or in a disparate manner to antagonize each other. It has been indicated that the two processes share common response machineries, including the B-cell lymphoma 2 (Bcl-2) family, reactive oxygen species, and intracellular calcium (15). Bcl-2 family proteins are classified as either anti-apoptotic or pro-apoptotic (16). For example, pro-apoptotic members of the Bcl-2 family accelerate apoptosis by antagonizing anti-apoptotic Bcl-2 proteins in several distinct ways (17). Typically, two major pro-apoptotic proteins, Bcl-2 antagonist killer 1 (Bak) and Bcl-2-associated x protein (Bax), accelerate mitochondrial outer membrane permeabilization via conformational changes and subsequent oligomerization on the mitochondrial membrane (18). The involvement of Bcl-2 family members or their interacting proteins in autophagy has recently been suggested because mammalian Beclin 1 has been demonstrated to be required for autophagy. Beclin 1 was initially identified as a Bcl-2-interacting protein, and its Bcl-2 homology domain 3 (BH3 domain) mediates interaction with Bcl-2 or Bcl-xL (19, 20). Similarly, it has been demonstrated that Bcl-2 family proteins influence autophagy mainly by regulating the interaction between Beclin 1 and Bcl-2/Bcl-xL (20–24). Nevertheless, the exact mechanisms underlying the regulatory roles for Bcl-2 family members still remain to be further delineated.

Nigericin is an ionophore and acts as an antiporter of K^+/H^+ and raises the pH of acidic compartments (25). In image-based screens for autophagy inducers, nigericin was identified as one of the candidates that increase LC3 spots following treatment (26). In addition, it has been reported that nigericin treatment reduces lysosomal protein degradation and inhibits fusion between autophagosomes and lysosomes by raising the pH of acidic compartments (27, 28). In our previous study using this ionophore, we demonstrated that Bax attenuates nigericin-induced MN9D dopaminergic neuronal cell death, although the exact mechanisms behind Bax-mediated regulation of cell death were not elucidated (29). Here, we primarily used MN9D dopaminergic neuronal cells to investigate (i) whether nigericin-induced neurodegeneration is accompanied by typical morphological and biochemical features of autophagy and (ii) whether and how Bak regulates nigericin-induced autophagic processes. In sum, we found that Bak attenuated nigericin-induced cell death potentially via its regulation of autophagic flux during ionophore-induced cell death.

EXPERIMENTAL PROCEDURES

Cell Culture and Drug Treatment—MN9D cells, N18TG cells, and HEK293 cells were cultured in Dulbecco's modified Eagle's medium (DMEM; Sigma) supplemented with 10% heat-inactivated fetal bovine serum (FBS) from Invitrogen. Culture medium was switched to serum-free N2 medium for drug treatment as described previously (30). Atg5 wild-type (WT) and knock-out (KO) MEF cells were cultured in DMEM supplemented with 10% FBS and 1% penicillin-streptomycin (Invitrogen). Cells were exposed to predetermined concentrations of nigericin (Sigma; 0.1, 0.5, 1, or 2.5 μM nigericin for MN9D, N18TG, HEK293, or MEF cells, respectively) for the indicated time periods. Other drugs used in the study included 1 μM staurosporine, 0.625 μM monensin, 10 μM chloroquine, and 10 mM ammonium chloride (all from Sigma), or 100 μM Z-VAD-fluoromethyl ketone (Enzyme System Products, Livermore, CA). All drug concentrations were empirically determined.

Construction of Eukaryotic Vectors and Transfection—Human full-length Bak was provided by Dr. J. C. Reed (Burnham Institute, La Jolla, CA). For construction of Myc-tagged Bak or FLAG-tagged Bak constructs, N-terminal Myc or FLAG tags were added to full-length human Bak cDNA by polymerase chain reaction (PCR; for Myc tag, 5′-GCC GGA TCC GCC ACC ATG GAA CAA AAG TTG ATT TCA GAA GAA GAT CTG GCC ATG GCA TCT GGA CAA GGA CCA G-3′; for FLAG tag, 5′- GCC GGA TCC GCC ACC ATG GAC TAT AAG GAC GAT GAT GAC AAG GCC ATG GCA TCT GGA CAA GGA CCA G-3′; for all, 3′-CGG AAT TCT CAT GAT CTG AAG AAT CTG TGT AC-5′). PCR products were digested with BamHI and EcoRI and ligated into the pcDNA3.1(+) vector. GFP-tagged LC3 cDNA was provided by Dr. Yoshimory (Osaka University). Transfection was performed using Lipofectamine 2000 (Invitrogen), as recommended by the supplier. The parent vector was used as a control. Stable cell lines overexpressing Myc-tagged (MN9D/m-Bak) or FLAG-tagged Bak (MN9D/f-Bak) were also established and characterized, as described previously (31). The stable cell lines were cultured in DMEM supplemented with 10% FBS and 500 μg/ml G-418 (A.G. Scientific, San Diego, CA). For gene silencing studies, two different pairs of siRNAs for human Bak (1011326 and 1011323 duplex) and negative siRNA (SN-1003) were purchased from Bioneer (Daejeon, Korea) and used for transfection. Each siRNA (50 nM) was transfected into the indicated cells using Lipofectamine 2000.

Electron Microscopy—As described previously in our laboratory (32), electron microscopic examination followed by quantitative analysis was performed after MN9D/neo, or MN9D/f-Bak cells were incubated with or without 0.1 μM nigericin. Briefly, ultrastructural examination of 80-nm thin sections was performed on a Hitachi H-7500 transmission electron microscope with 80-kV acceleration voltage. Quantitative analysis of the electron photomicrographs for the average numbers of autophagic vacuoles (AVs) per cell and areas occupied by swollen vacuoles was conducted using Scion Image software (Scion Corp.). All quantitative analyses were calculated from 30 randomly selected cells in two independent experiments.

Fluorescence and Phase-contrast Microscopy—After incubation with nigericin for the indicated time periods, cells were fixed with 4% paraformaldehyde (EMS, Hatfield, PA) for 15 min and then permeabilized with 0.1% saponin (Sigma) for 10 min at room temperature. Cells were then blocked in phosphate-buffered saline (PBS; Lonza, Basel, Switzerland) containing 0.2% Triton X-100 and 5% normal goat serum (Invitrogen). Cells were then incubated with rabbit anti-LC3 antibody (1:200; Cell Signaling, Beverly, MA) or mouse anti-Lamp1 antibody (1:200; Developmental Studies Hybridoma Bank, Iowa City, IA) in PBS containing 0.2% Triton X-100 and 1% normal goat serum overnight at 4 °C. After extensive washing with PBS, cells were incubated with Alexa 488-conjugated goat anti-rabbit IgG or Alexa 488-conjugated goat anti-mouse IgG (1:200; all from Invitro-

gen) at room temperature for 1 h. Nuclei were stained with Hoechst 33258 (1 μg/ml; Molecular Probes, Inc., Eugene, OR) for 10 min at room temperature, and slides were mounted in Vectashield mounting medium (Vector Laboratories, Burlingame, CA). Images were acquired under an LSM 510 META confocal laser-scanning microscope equipped with epifluorescence and a digital image analyzer (Carl Zeiss, Zena, Germany). As previously described by us (32), acquired images were analyzed for LC3 spots using MetaMorph (Molecular Devices, Downingtown, PA). Each Z series was maximum-projected and then used for quantitation of areas and numbers of LC3 spots per cell. Thirty randomly selected cells from three independent experiments were subjected to quantitative analysis. To obtain live images of GFP-tagged LC3, cells treated with or without 0.1 μM nigericin for the indicated time periods were washed with PBS and photographed under an Axio Observer A1 microscope (Carl Zeiss).

Immunoblot Analysis—Following drug treatment, MN9D, N18TG, HEK293, or MEF cells were lysed with radioimmune precipitation buffer and processed as described previously (32). The primary antibodies used included rabbit anti-LC3 (1:4,000; Cell Signaling), guinea pig anti-p62 (1:5,000; Progen Biotechnik, Heidelberg, Germany), rabbit anti-cleaved caspase-3 (1:1,000; Cell signaling), mouse anti-Myc antibody (1:2,000; Cell Signaling), rabbit anti-Bak (1:1,000; Upstate, Lake Placid, NY), rabbit anti-GFP (1:1,000; Santa Cruz Biotechnology, Inc., Santa Cruz, CA), rabbit anti-Atg5 (1:3,000; Abcam, Cambridge, MA), and HRP-conjugated anti-FLAG (1:5,000; Sigma). Duplicate blots probed with mouse anti-GAPDH (1:4,000; Chemicon, Dundee, UK) or rabbit anti-actin (1:3,000; Sigma) were used as loading controls. After incubation with primary antibody, membranes were washed with Tris-buffered saline containing 0.1% Tween 20, followed by incubation with the appropriate horseradish peroxidase-conjugated anti-rabbit (1:4,000; Santa Cruz Biotechnology, Inc.), anti-mouse (1:4,000; Santa Cruz Biotechnology, Inc.), or anti-guinea pig antibody (1:4,000; Sigma). Specific bands were visualized using the enhanced chemiluminescence kit (PerkinElmer Life Sciences). After measuring the intensity of each band by densitometry using ImageJ, relative intensities were calculated by normalizing to GAPDH from the corresponding sample.

Activity and Viability Assays—Following nigericin treatment, MN9D cells were lysed with the InnoZyme^{TM} cathepsin L activity kit (Calbiochem), as recommended by the supplier. Cell lysates were then incubated with fluorogenic substrate Z-Phe-Arg-7-amido-4-methylcoumarin for 1 h at 37 °C. For measurement of mitochondrial membrane potential, cells were incubated with 250 nM Mitotracker Orange CMXRos (Invitrogen) for 30 min at 37 °C and then washed twice with PBS. Fluorescence intensity was measured at Ex360/Em460 nm (excitation/emission wave length for cathepsin activity) or at Ex554/Em576 nm (for Mitotracker Orange) using a FL600 microplate reader (BioTek, Winooski, VT). Nigericin-treated MN9D cells were subjected to FACS analysis of Annexin V binding and propidium iodide uptake using the FITC Annexin V Apoptosis Detection Kit 1 (BD Biosciences). Cells were stained with propidium iodide/Annexin V as per the supplier's instructions and analyzed on a FACSCalibur (BD Biosciences). The percentage of cells in each quadrant over the total number of the counted cells was calculated using CellQuest (BD Biosciences). Following drug treatment, the rate of cell viability was measured by the 3-(4,5-dimethylthiazol-2-yl)-2,5-diphenyltetrazolium bromide (MTT) reduction assay, as described previously (33). Phase-contrast photomicrographs were taken with an Axio Observer A1 microscope (Carl Zeiss).

Statistics—Data are presented as the mean ± S.D. from three independent experiments, unless otherwise indicated. Student's *t* tests were used for determining significant differences between groups. Values of $p < 0.001$ or $p < 0.05$ were considered statistically significant.

RESULTS

Characterization of Nigericin-induced MN9D Neuronal Cell Death—To unequivocally characterize and quantify nigericin-induced cell death, we performed multiple, methodologically unrelated assays, as previously described (10). First, we examined the morphological changes of MN9D cells treated with or without nigericin for 12 h under a phase-contrast microscope. As shown in Fig. 1*A*, nigericin induced the dramatic accumulation of vacuole-like structures in the cytosol. As determined by MTT reduction assays, the viability of MN9D cells decreased following nigericin treatment in a time-dependent manner (Fig. 1*B*). Quite similar patterns were obtained by a colorimetric measurement using a well known vital staining dye, neural red (71.2 ± 6.8% at 12 h, and 39.3 ± 10.6% at 18 h over the untreated control cells; $n = 3$, $p < 0.05$). Next, we monitored double staining patterns of FITC-conjugated Annexin V and propidium iodide by FACS. Our FACS analysis revealed that nigericin-induced cell death produced a mixture of population positive for Annexin V alone and population positive for both Annexin V and propidium iodide (Fig. 1*C*). Analyses with Mitotracker Orange indicated a collapse of mitochondrial potential ($\Delta\Psi$) following nigericin treatment (Fig. 1*D*). Immunoblot analyses using antibodies recognizing a cleaved caspase-3 revealed that caspase-3 activity increased following nigericin treatment (Fig. 1*E*). Co-treatment of cells with Z-VAD-fluoromethyl ketone (a pan-caspase inhibitor) blocked nigericin-induced cell death (Fig. 1*F*). Similarly, a neutral red-based colorimetric assay demonstrated that a caspase inhibitor attenuates drug-induced cell death (at 18 h, 39.3 ± 10.6% for nigericin alone *versus* 67.2 ± 9.4% for nigericin plus Z-VAD; $n = 3$, $p < 0.05$).

Characterization of Autophagic Events following Nigericin Treatment—Based on previous reports by others (26–28), we hypothesized that nigericin-induced cell death may also recruit autophagic events. To directly test this, we first examined ultrastructural changes in MN9D cells before and after nigericin treatment. Based on the previous report describing in detail ultrastructural criteria and characterization to monitor autophagy (34), we identified four important structures: autophagosome, autolysosome, swollen endosome, and MVB. We found that MN9D cells exposed to nigericin for 7 h underwent dramatic morphological changes (Fig. 2*A*, *top panels*). The presence of AVs that are typical of autophagy was found within the cytosol (Fig. 2*A*, *bottom left panels*). Quantitative analyses indicated that the numbers of AVs increased following

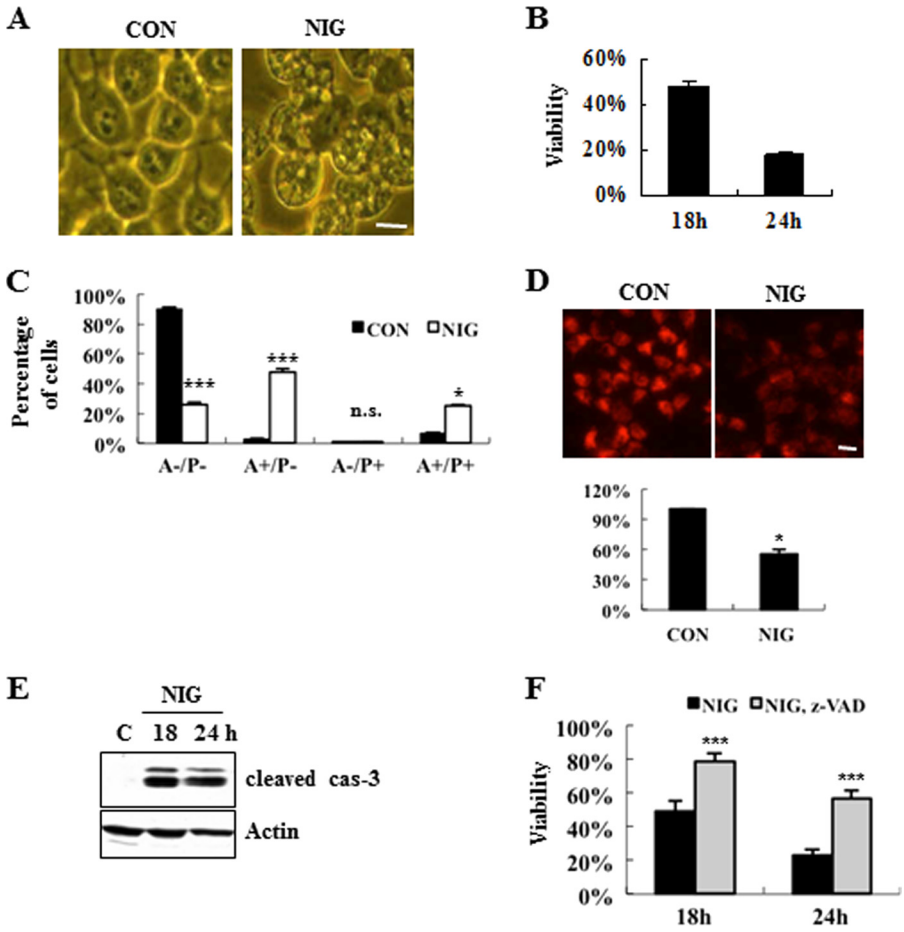

FIGURE 1. **Characterization of nigericin-induced MN9D neuronal cell death.** Multiple assays were performed to quantify nigericin-induced neuronal cell death as described previously (10). *A*, phase-contrast images of MN9D cells incubated for 12 h with 0.1 μM nigericin (*NIG*) or without drug (*CON*). *Scale bar*, 10 μm. *B*, MTT reduction assays were performed following 0.1 μM nigericin treatment for the indicated time periods. Viability after each treatment was expressed as a percentage over the untreated control cells (100%). Each point represents the mean ± S.D. (*error bars*) from three independent experiments done in triplicate. *C*, FACS analysis on Annexin V (*A*) and propidium iodide (*P*) was performed following treatment with 0.1 μM nigericin for 18 h. Values from FACS analysis were shown as a percentage of the cell numbers from each quadrant over the total number of the counted cells from three independent experiments. *D*, to measure the mitochondrial membrane potential, MN9D cells were loaded with 250 nM Mitotracker Orange CMXRos after incubation with or without 0.1 μM nigericin. Fluorescence photomicrographs were taken at 18 h after nigericin treatment under a confocal microscope. *Scale bar*, 10 μm. The relative intensity was quantified using a microplate reader and expressed as a percentage of the untreated control cells (100%). *Bar*, mean ± S.D. from three independent experiments in triplicate. *E*, following nigericin treatment, caspase-3 activities were assessed by immunoblot analysis using anti-cleaved caspase-3. Actin was used as a loading control. *F*, viability was measured by the MTT reduction assay after exposure to 0.1 μM nigericin alone or in combination with 100 μM Z-VAD-fluoromethyl ketone for the time periods indicated. Viability was expressed as a percentage over the untreated control cells (100%). *Bar*, mean ± S.D. from three independent experiments in triplicate. *, $p < 0.05$; ***, $p < 0.001$; *n.s.*, not significant.

nigericin treatment (Fig. 2*A*, *bottom right panel*). In addition, the appearance of swollen vacuoles (*black arrows*) was detected, which is presumably related to endosomal systems (35). Next, we attempted to check the involvement of autophagy during nigericin-induced cell death on a biochemical level, and we performed immunoblot analysis using an antibody that recognizes LC3. Fig. 2*B* shows that nigericin treatment induced accumulation of the endogenous LC3-II form. Due to localization of LC3-II at the autophagosomal vesicles, the formation and punctated staining pattern of LC3-II forms are also widely used to monitor autophagy. To effectively visualize its punctated staining pattern, we used saponin as a permeabilizing reagent that removes soluble LC3 proteins from the cells and efficiently leaves the membrane-associated form of LC3 proteins within the cytosol. As shown in Fig. 2*C*, immunocytochemical localization analysis revealed that a prominently punctated staining pattern for LC3 was detected in cells treated with nigericin (*right panel*). Quantitative analyses demonstrated that the total area of LC3 spots as well as the numbers of LC3 punctated spots increased after nigericin treatment for 12 h (Fig. 2*D*). Similarly, we observed a punctated staining pattern for exogenous GFP-tagged LC3 from live cell fluorescence images (Fig. 2*E*) and an accumulation of GFP-LC3-II (Fig. 2*F*) in nigericin-treated MN9D cells stably transfected with a eukaryotic vector containing GFP-tagged LC3 cDNA. Collectively, our data demonstrated that both apoptotic and autophagic events were induced during nigericin-mediated cell death. As shown in supplemental Fig. S1, however, co-treatment with Z-VAD did not affect the nigericin-induced levels of LC3-II, implying that nigericin-induced apoptotic signal may not be linked to autophagic events.

Impaired Autophagic Flux following Nigericin Treatment—Using lysomotropic agents, such as chloroquine and ammonium chloride, that inhibit protein degradation by raising

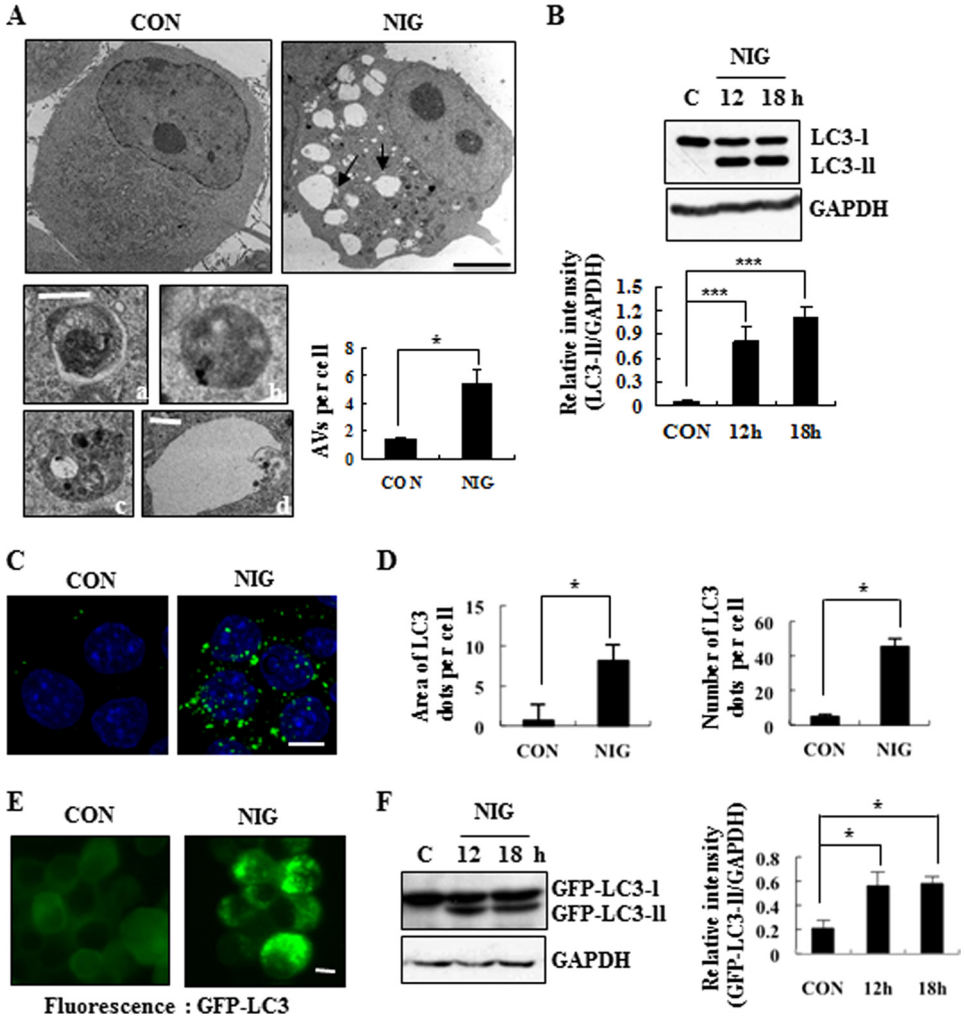

FIGURE 2. **Ultrastructural and biochemical characterization of nigericin-induced MN9D neuronal cell death.** *A*, representative electron micrographs of MN9D cells treated for 7 h with (*NIG*) or without (*CON*) 0.1 μM nigericin. *Black scale bars*, 5 μm. Swollen vacuoles in nigericin-treated cell are indicated by *black arrows*. Ultrastructural identification of AVs (autophagosome and autolysosome) appeared in MN9D cells was basically made by the guideline provided in the previous work (34). *Enlarged images* of typical autophagosome (*a*), autolysosome (*b*), MVB (*c*), and swollen endosome (*d*) frequently found in nigericin-treated cells are shown in the *left*, *bottom panels*. *White scale bars*, 250 nm. The average numbers of AVs per cell were quantified from 30 randomly selected cells from two independent experiments. *Bars*, average numbers of AVs per cell. *B*, levels of LC3-II were assessed by immunoblot analysis using anti-LC3 antibody after incubation with or without 0.1 μM nigericin. GAPDH was used as a loading control. Densitometric analysis was performed using ImageJ. The relative intensity of LC3-II in each sample was calculated after normalization to GAPDH in the corresponding sample. Each *bar* represents the mean ± S.D. (*error bars*) from three independent experiments. *C*, confocal immunofluorescence images after immunocytochemistry using anti-LC3 antibody in cells treated for 12 h with or without 0.1 μM nigericin. Saponin was used to permeabilize the cells to remove the soluble proteins in the cytosol. Nuclei were stained with 1 μg/ml Hoechst 33258. *Scale bar*, 10 μm. *D*, average area and number of LC3 spots per cell were quantified as described under "Experimental Procedures." Thirty cells from each of three independent experiments were quantified. *E*, representative live images from MN9D cells stably expressing GFP-LC3 before and after nigericin treatment for 12 h. *Scale bar*, 10 μm. *F*, the level of GFP-LC3-II was assessed through immunoblot analysis using anti-GFP antibody. GAPDH was utilized as a loading control. The relative intensity of LC3-II in each sample was calculated after normalization to GAPDH in the corresponding sample. Each *bar* represents the mean ± S.D. from three independent experiments. *, $p < 0.05$; ***, $p < 0.001$.

intralysosomal pH (36), we specifically investigated whether the nigericin-induced accumulation of LC3-II is due to enhanced synthesis or reduced degradation. When we compared and quantitated the levels of LC3-II in nigericin-treated cells in the presence or absence of chloroquine or ammonium chloride, we found that co-treatment with lysomotropic agents did not lead to further increase in nigericin-induced accumulation of LC3-II (Fig. 3*A*), suggesting that accumulation of LC3-II was most likely caused by an impairment of autophagic flux. p62/SQSTM1 is widely used to monitor autophagy, due to its localization at the autophagic compartments and subsequent degradation through autophagy (37). Immunoblot analysis demonstrated that nigericin treatment increased the level of p62/SQSTM1 over 18 h, supporting the notion that nigericin impaired the autophagic degradation process (Fig. 3*B*). To determine which step may be responsible for the compromised autophagy, we monitored the total cathepsin activity in an *in vitro* cathepsin substrate assay. As shown in Fig. 3*C*, nigericin caused a reduction of cathepsin activity in MN9D cells. Moreover, immunocytochemical localization studies showed that the signal from Lamp1 was diminished following nigericin treatment compared with control cells (Fig. 3*D*), implying that nigericin may lead to lysosomal dysfunction. To compare viability and expression patterns of LC3-II and p62, we also utilized Atg5 WT and KO MEF cells (Fig. 4*A*). We found that nigericin-induced cell death was accelerated in Atg5 KO MEF

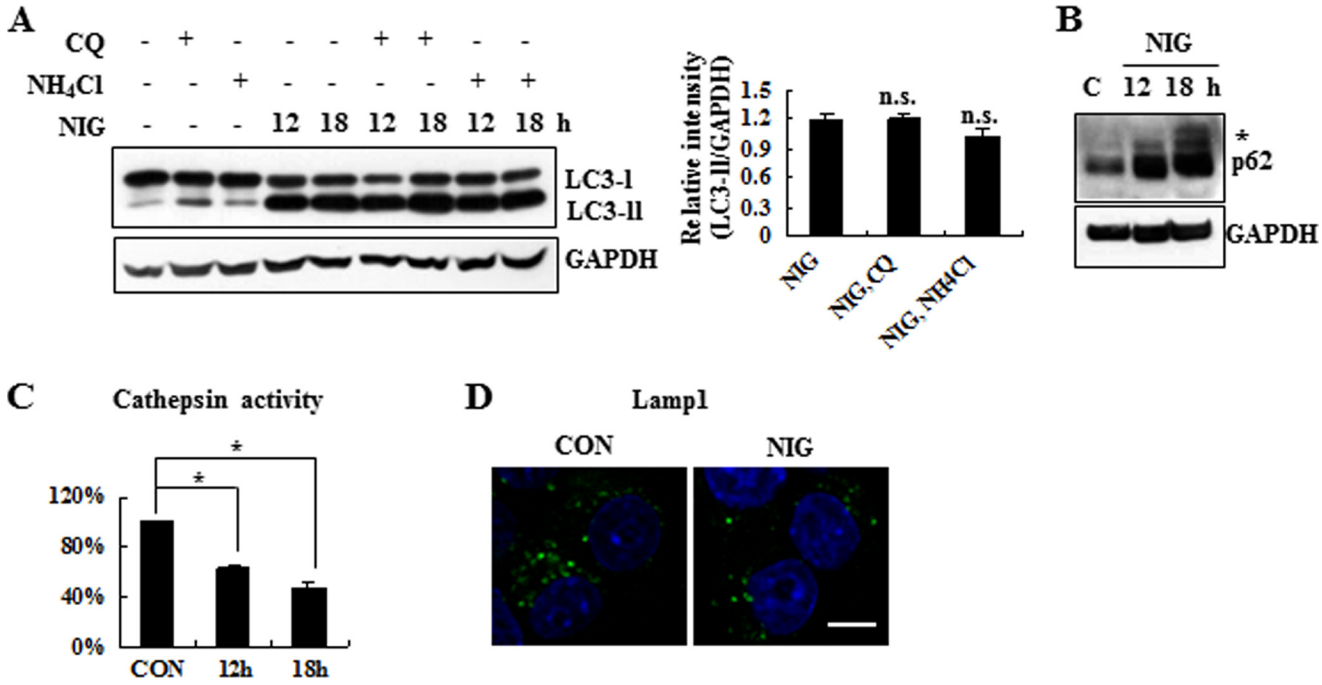

FIGURE 3. **Impaired autophagic flux during nigericin-induced MN9D neuronal cell death.** *A*, autophagic flux was monitored in cell lysates exposed to 0.1 μM nigericin for the time periods indicated in the presence or the absence of 10 μM chloroquine (CQ) or 10 mM ammonium chloride (NH_4Cl). Relative intensity of LC3-II normalized to GAPDH was calculated. Each *bar* represents the mean ± S.D. (*error bars*) from three independent experiments. *B*, following treatment with 0.1 μM nigericin for the indicated time periods, immunoblot analysis was performed to detect protein levels of p62. GAPDH was used as a loading control. An *asterisk* indicates modified forms of p62. *C*, *in vitro* cathepsin activity assays were performed, as described under "Experimental Procedures." Values are expressed as a percentage of the untreated control cells (100%). Each *bar* represents the mean ± S.D. from three independent experiments. *D*, MN9D cells treated with or without 0.1 μM nigericin for 18 h were subjected to immunocytochemical analysis using anti-Lamp1 antibody. Representative confocal images are provided. *Scale bar*, 10 μm. *, $p < 0.05$; *n.s.*, not significant.

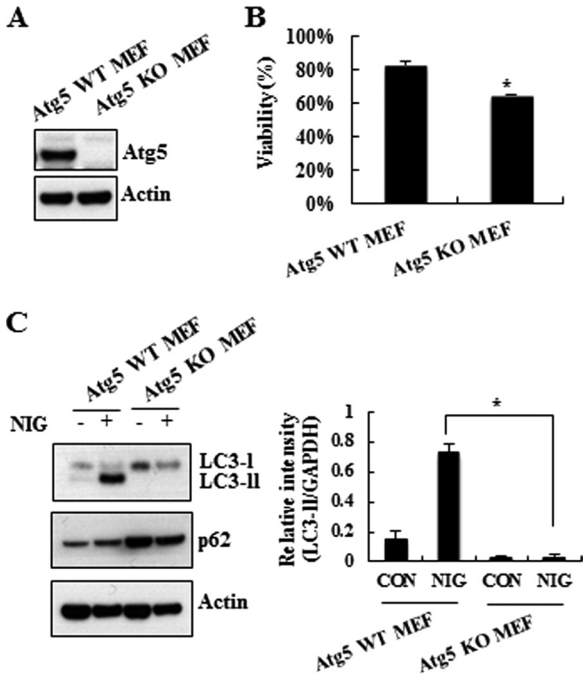

FIGURE 4. **Effect of Atg5 knock-out on the rate of cell viability and levels of LC3-II and p62.** *A*, cell lysates from Atg5 WT MEF and Atg5 KO MEF cells were probed with anti-Atg5 antibody. Actin was used as a loading control. *B*, MTT reduction assay was carried out following 2.5 μM nigericin treatment for 24 h. Viability is expressed as a percentage over the untreated control cells (100%) from three independent experiments in triplicate. *C*, immunoblot analysis was then performed using anti-LC3, -p62, and -actin antibodies. Relative intensity of LC3-II in each condition was calculated and compared, as described above. *, $p < 0.05$. *Error bars*, S.D.

cells compared with that in Atg5 WT MEF cells (Fig. 4*B*). As expected, LC3-II was hardly seen, and an increased level of p62 was found in Atg5 KO MEF cells (Fig. 4*C*). Taken together, our data suggest that autophagy is associated with nigericin-induced cell death, and, most importantly, impairment of autophagic flux presumably through lysosomal dysfunction is responsible for nigericin-induced cell death.

Bak-mediated Attenuation of Nigericin-induced Cell Death—Based on our previous studies, demonstrating a dual role for the pro-apoptotic Bcl-2 family in protecting cells from nigericin-induced cell death while accelerating staurosporine-induced cell death (29), we tested whether and how Bak exerts a protective role in these cell death paradigms. First, we conducted MTT reduction assays in staurosporine- or nigericin-treated MN9D cells, transiently or stably transfected with a vector encoding human Bak cDNA or empty vector as a control. When MN9D cells transiently or stably transfected with Bak were exposed to staurosporine for 18 h, they were more vulnerable to the cell death-inducing stimuli (supplemental Fig. S2). In contrast, MN9D cells transiently overexpressing Bak were ~20% more resistant to cell death following treatment with nigericin (Fig. 5, *A* and *B*). This protective effect of Bak was consistently reproduced in nigericin-treated MN9D cells stably overexpressing Myc-tagged or FLAG-tagged Bak (Fig. 5, *C* and *D*). To determine if the protective role for Bak was cell type-specific, N18TG neuroglioma cells stably transfected with or without Bak were exposed to nigericin and subjected to the MTT reduction assays. As shown in Fig. 5, *E* and *F*, two independent lines overexpressing Bak signif-

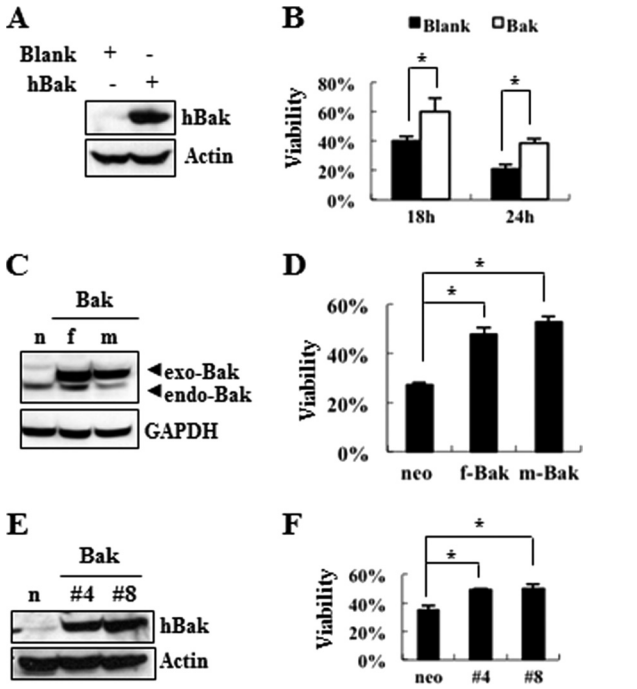

FIGURE 5. **Attenuation of nigericin-induced cell death by overexpressed Bak.** After transient transfection of MN9D cells with an expression vector encoding human Bak (*A*), stable transfection of MN9D cells with empty vector (*n*) and a vector encoding either FLAG-tagged human Bak (*f*) or Myc-tagged Bak (*m*) (*C*), and stable transfection of N18TG cells with empty vector (*n*) or human Bak (*E*), protein levels were detected by immunoblot analysis using anti-Bak antibody. GAPDH or actin was used as a loading control. *B*, *D*, and *F*, MTT reduction assay was carried out following 0.1 μM nigericin treatment for 18 and 24 h (*B*) or 24 h (*D* and *F*). Viability after each treatment is expressed as a percentage over the untreated control cells (100%) from three independent experiments in triplicate. *, $p < 0.05$. *Error bars*, S.D.

icantly protected N18TG cells from nigericin-induced death.

Inhibitory Role of Bak in Nigericin-mediated Accumulation of LC3-II—To determine the underlying protective mechanism exerted by Bak, we compared the levels of the cleaved form of caspase-3 and LC3-II in nigericin-treated or non-treated MN9D cells stably overexpressing control empty vector or FLAG-tagged or Myc-tagged Bak (MN9D/neo, MN9D/f-Bak, or MN9D/m-Bak, respectively). Immunoblot analyses of these stable cell lines showed that nigericin-induced caspase activity was similar or slightly increased in two independent stable cell lines overexpressing Bak (Fig. 6*A*). In contrast, there was a significant difference in the levels of LC3-II between nigericin-treated MN9D/neo and the two MN9D/Bak stable cell lines. Quantitative analysis revealed that the relative intensities of LC3-II over GAPDH were significantly diminished in the two independent MN9D/Bak cell lines after treatment with nigericin for 12 and 18 h (Fig. 6*A*, *bottom panel*). In support of this finding, in an immunocytochemical localization study, reduced levels of LC3 spots were detected in MN9D/f-Bak cells following nigericin treatment (Fig. 6*B*, *top panels*). Quantitative analyses demonstrated a significant reduction in the areas occupied by LC3 spots and the total numbers of punctated LC3 spots per cell in nigericin-treated MN9D/f-Bak cells (Fig. 6*B*, *bottom panels*). This phenomenon was reproduced when MN9D cells transiently transfected with Bak were exposed to nigericin and subjected to immunoblot analysis of LC3 (Fig. 6*C*) and subsequent quantitative analysis (Fig. 6*D*). Furthermore, nigericin-induced accumulation of p62 was inhibited in Bak-overexpressing cells (Fig. 6, *C* and *D*). To confirm that this effect is genuinely caused by Bak, we established human embryonic kidney HEK293 and MN9D cells transfected with control siRNA or siRNA targeting human Bak mRNA. When we first compared the relative intensities of LC3-II over GAPDH in HEK293 cells treated with or without nigiricin, we found that knockdown of endogenous Bak increased the level of LC3-II, whereas overexpression of human Bak diminished the relative intensity of LC3-II (Fig. 7, *A* and *B*). Because MN9D cells express quite low levels of endogenous Bak, we first established MN9D cells transiently overexpressing FLAG-tagged Bak and then targeted the exogenous Bak via two independent Bak siRNAs (*#1* and *#2* in Fig. 7*C*). As shown in Fig. 7*C*, the levels of LC3-II in Bak siRNA-transfected MN9D cells were significantly increased compared with negative siRNA-transfected MN9D cells following nigericin treatment. Taken together, our data indicate that Bak attenuated the nigericin-induced accumulation of LC3-II in both neuronal and non-neuronal cells and that its inhibitory effect seemed to be independent of caspase activity.

Bak Attenuates Nigericin-induced Cell Death through Regulating Autophagic Flux—Next, we examined whether the Bak-mediated reduction of LC3-II was a consequence of inhibiting autophagy induction or of accelerating autophagic flux. Toward this end, we treated MN9D/neo and MN9D/f-Bak cells with nigericin in the presence or absence of chloriquine and subsequently performed immunoblot analysis to measure the levels of LC3-II. Exposure of MN9D/f-Bak cells to nigericin in the presence of chloroquine tremendously increased the levels of LC3-II, compared with MN9D/f-Bak cells treated with nigericin alone (Fig. 8*A*). Although treatment of chloroquine alone only slightly increased the basal level of LC3-II (refer to Fig. 3*A*), co-treatment with nigericin significantly increased LC3-II, indicating a synergic effect of chloroquine in MN9D/f-Bak cells. Furthermore, the relative intensity of nigericin-induced LC3-II was similar in both MN9D/neo and MN9D/f-Bak at 18 h, in the presence of chloroquine. This phenomenon was reproduced when we treated cells with nigericin in combination with another lysomotropic agent, ammonium chloride (data not shown). We next investigated whether Bak is critically involved in the maintenance of autophagic flux during cell death induced by agents that have properties similar to those of nigericin. The structure and properties of nigericin are similar to those of monensin, although monensin has a preference for Na^+ instead of K^+ (25, 38). Like nigericin, monensin treatment disrupts lysosomal function (27, 39). Immunoblotting with anti-LC3 antibody and quantitative analysis showed that the time-dependent increase in LC3-II following monensin treatment was not exacerbated by the presence of chloroquine, indicating that monensin also impaired autophagic flux in MN9D cells (supplemental Fig. S3, *A* and *B*). MTT reduction assays indicated that monensin-induced cell death was attenuated in MN9D cells stably overexpressing Bak (supplemental Fig. S3*C*). In these MN9D/m-Bak cells, the rate of monensin-induced accumulation of LC3-II was further increased in the presence of chloroquine (supplemental Fig. S3*D*). As shown in supplemental Fig. 3*E*, the relative intensity of monensin-induced LC3-II

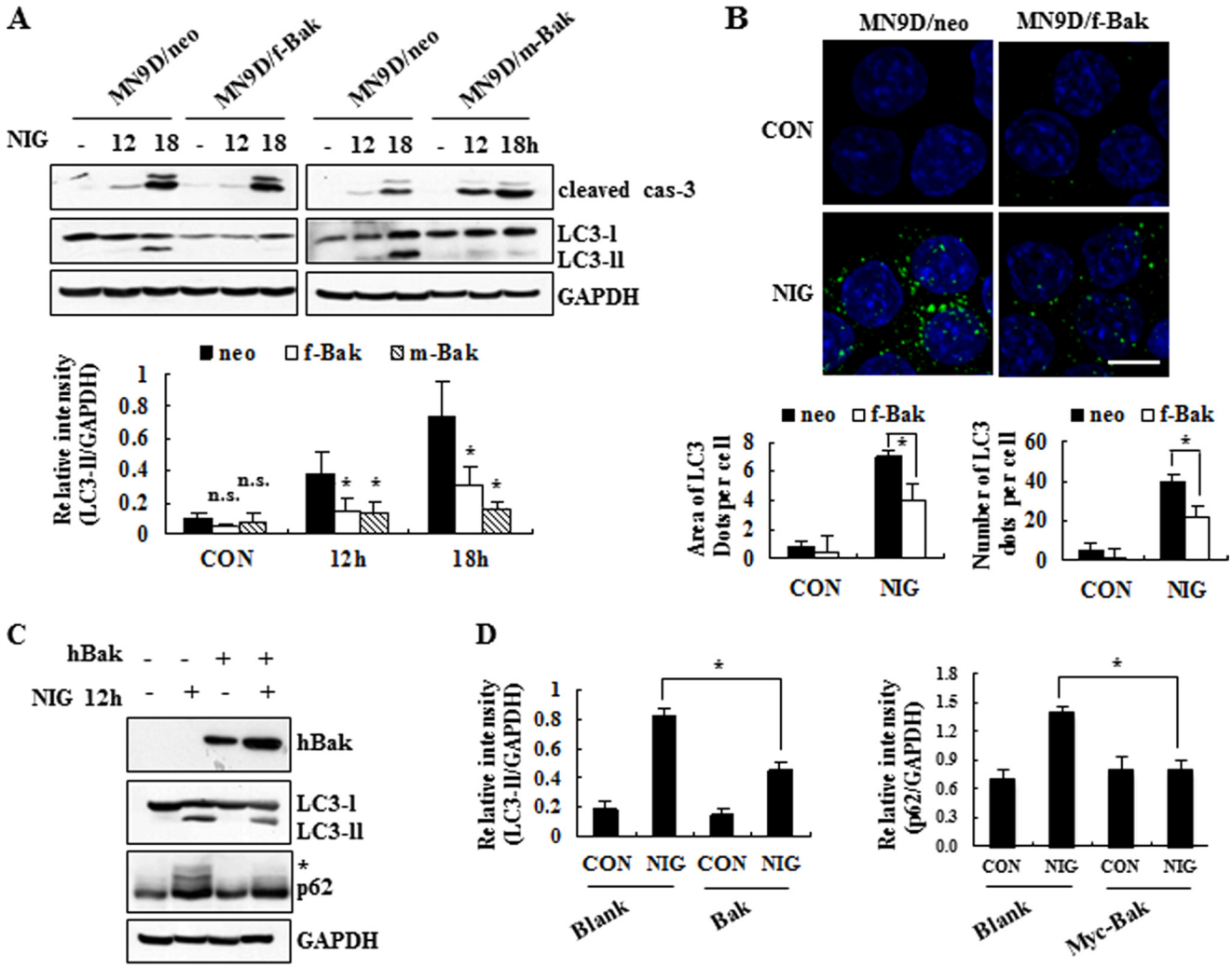

FIGURE 6. **Bak hinders nigericin-induced accumulation of LC3-II.** *A*, representative blots of stable cell lines overexpressing an empty vector (MN9D/neo), FLAG-tagged Bak (MN9D/f-Bak), or Myc-tagged Bak (MN9D/m-Bak) were shown. Following exposure to 0.1 μM nigericin for the indicated time periods, cell lysates were harvested, transblotted, and probed with antibodies that recognize the cleaved caspase-3, LC3, and GAPDH, respectively. GAPDH was used as a loading control. Relative intensity of LC3-II normalized to GAPDH was calculated after densitometric analysis using ImageJ (*bottom*). *B*, using anti-LC3 antibody, confocal immunofluorescence images of MN9D/neo and MN9D/f-Bak were obtained after treatment with or without 0.1 μM nigericin for 12 h. *Scale bar*, 10 μm. The average area and number of LC3 spots per cell were measured using Metamorph and determined as described in the legend to Fig. 2*C*. *C*, MN9D cells were transiently transfected with empty vector (−) or human Bak (+) and then exposed to 0.1 μM nigericin for 12 h. Subsequently, cells were lysed and probed with anti-Bak, -LC3, -p62, and -GAPDH antibodies. An *asterisk* indicates modified forms of p62. *D*, relative intensity of LC3-II and p62 in each cell line was calculated and compared, as described above. *A*, *B*, and *D*, all values for quantitative analyses represent the mean ± S.D. (*error bars*) from three independent experiments. *, $p < 0.05$; *n.s.*, not significant.

was also similar in both MN9D/neo and MN9D/m-Bak cells at 18 h, in the presence of chloroquine. Collectively, these results support the notion that Bak seems to attenuate carboxylic ionophore-induced cell death by maintaining autophagic flux. Interestingly, we found that the rate of nigericin-induced decrease of cathepsin activity was similar both in MN9D/neo and MN9D/Bak cells (supplemental Fig. S4), suggesting that Bak may maintain autophagic flux not by directly affecting lysosomal enzymatic activity but by other important steps of autophagic events. Next, we monitored the ultrastructural changes in MN9D/neo and MN9D/f-Bak cells after treatment with or without nigericin. At 9 h, a slight difference in the numbers of AVs (*white arrows*) was detected in both MN9D/neo and MN9D/m-Bak cells. However, a large amount of swollen vacuoles appeared in the cytosol of MN9D/neo cells (Fig. 8*B*, *black arrows*). As indicated previously by Thorens and Roth (35), the appearance of these swollen vacuoles seemed to be related to endosomal systems. On the other hand, swollen vacuoles were less frequently observed in nigericin-treated MN9D/f-Bak cells. Quantitative analysis of the electron micrographs further revealed that the area occupied by the swollen vacuoles in MN9D/f-Bak cells was significantly smaller than in MN9D/neo cells following nigericin treatment (Fig. 8*C*). Taken together, we are tempted to argue that Bak may actively regulate the vacuolar systems that are abnormally swollen during nigericin-induced cell death, and this activity may be involved in maintaining autophagic flux during nigericin-induced cell death.

DISCUSSION

Ultrastructural examination indicates that nigericin induces severe vacuolization in the cytosol, including autophagic vacu-

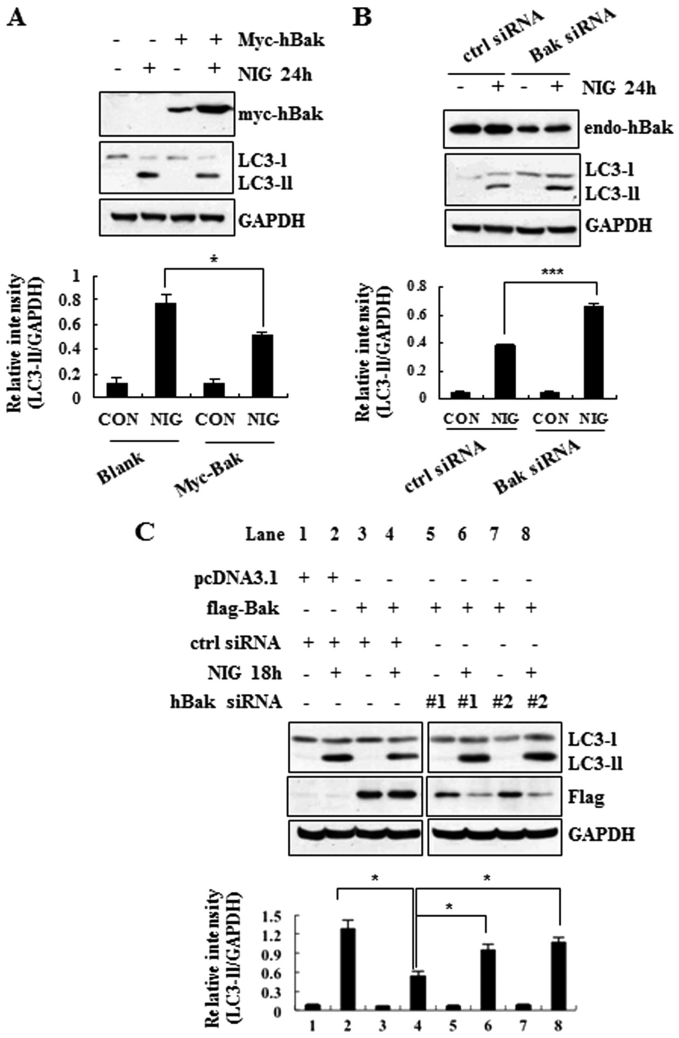

FIGURE 7. **Knockdown of Bak accelerates nigericin-induced accumulation of LC3-II in HEK293 and MN9D cells.** *A* and *B*, after 48 h of transient transfection with Myc-tagged human Bak (*A*) and negative (*ctrl*) siRNA or Bak siRNA (*B*), HEK293 cells were treated with or without 1 μM nigericin for 24 h. Immunoblot analysis was then performed with anti-Myc, -Bak, -LC3, and -GAPDH antibodies. Relative intensity of LC3-II in each condition was calculated and compared, as described above. *C*, after 24 h of transfection with empty vector (pcDNA3.1) or a vector encoding FLAG-human Bak, MN9D cells were further transfected with negative siRNA or two distinct sets of siRNAs targeting human Bak sequences (*hBak*). After 24 h post-transfection, MN9D cells were treated with 0.1 μM nigericin for 18 h and subjected to immunoblot analysis with anti-LC3, -FLAG, or -GAPDH antibodies. Relative intensity of LC3-II normalized to GAPDH in each condition was calculated and compared. *A–C*, All values from quantitative analyses represent the mean ± S.D. (*error bars*) from three independent experiments. *, $p < 0.05$; ***, $p < 0.001$.

oles and swollen vacuoles. Immunological analyses using anti-LC3 antibody show increase in LC3-II and a punctated staining pattern in nigericin-treated cells, demonstrating that nigericin induces MN9D neurodegeneration, morphologically and biochemically typical of autophagy. Furthermore, our data for such lysomotropic agents as chloroquine and ammonium chloride support the notion that the nigericin-induced accumulation of LC3-II is due to impaired autophgic flux. We found that treatment with another ionophore, monensin, that is structurally and functionally related to nigericin, also impairs autophagic flux in MN9D cells. Based on our data from an *in vitro* cathepsin substrate assay and from immunocytochemical localization of Lamp1, we propose that lysosomal dysfunction may be responsible for nigericin-induced impairment of autophagic flux.

In this death paradigm, our data indicate that exogenous expression of Bak reverses these phenomena. Consistent with our previously published data showing a dual role for Bax (29), for example, we demonstrate that Bak also renders a resistance to nigericin-induced cell death and inhibits drug-induced accumulation of LC3-II. Moreover, the inhibitory role for Bak is found in N18TG and HEK cells, indicating that its unusual protective role is not cell type-specific. This inhibitory activity of Bak is carefully confirmed in various experimental conditions, including cells transiently or stably transfected with expression vectors encoding one of several types of Bak or in Bak-silenced cells, indicating that Bak is indeed responsible for the inhibition of nigericin-induced appearance of vacuoles, accumulation of LC3-II, and subsequent cell death. Although accumulating evidence supports a protective role of autophagy in diverse conditions, immature completion of the autophagic process can also lead to the impairment of autophagic flux, and this event is in turn linked to cell death (40). In this study, data from co-treatment with chloroquine and ultrastructural examination in Bak-overexpressing cells indicate that its inhibitory role may be closely associated with its regulatory effect on maintaining autophagic flux. Considering that maturation of lysosomes requires the functional endosomal system (41, 42), Bak may block nigericin-induced generation of swollen vacuoles via inhibiting drug-induced impairment of the formation of late endosome or lysosome compartments. However, this possibility has to be thoroughly investigated.

There have been a few studies, including ones from our laboratory, that have revealed that Bax and Bak delay or protect against cell death, depending on specific stimuli or developmental stages (29). Typically, Bax and Bak promote apoptosis through inducing mitochondrial outer membrane permeabilization to release pro-apoptotic molecules from the mitochondria and causing excessive release of ER calcium (17, 43). Indeed, we here demonstrate that transient or stable overexpression of Bak accelerates staurosporine-induced MN9D cell death, whereas it blocks nigericin-induced cell death. Etoposide-induced apoptotic cell death is also accelerated in Bak-overexpressing MN9D cells.[3] This phenomenon is recapitulated in other cell types, including N18TG cells, implying a dual role for Bak in these distinct cell death paradigms. In consideration of our data demonstrating that treatment of a pan-caspase inhibitor does not affect the nigericin-induced accumulation of LC3-II and overexpressed Bak does not block nigericin-induced levels of the cleaved caspase-3 in MN9D cells, it is highly likely that the protective role for Bak in nigericin-induced cell death is independent of caspase activity. In contrast to what we expected, our unpublished data[3] indicate that the protective function of Bak during nigericin-induced cell death is also attributable to its BH3 domain, which has been demonstrated to be critical for exerting its pro-apoptotic activity. Although it has not been carefully determined whether deletion of the BH3 domain also abolishes Bak-mediated inhibition of LC3-II accu-

[3] Y. Lee, J. Lim, I. J. Rhyu, and Y. J. Oh, unpublished data.

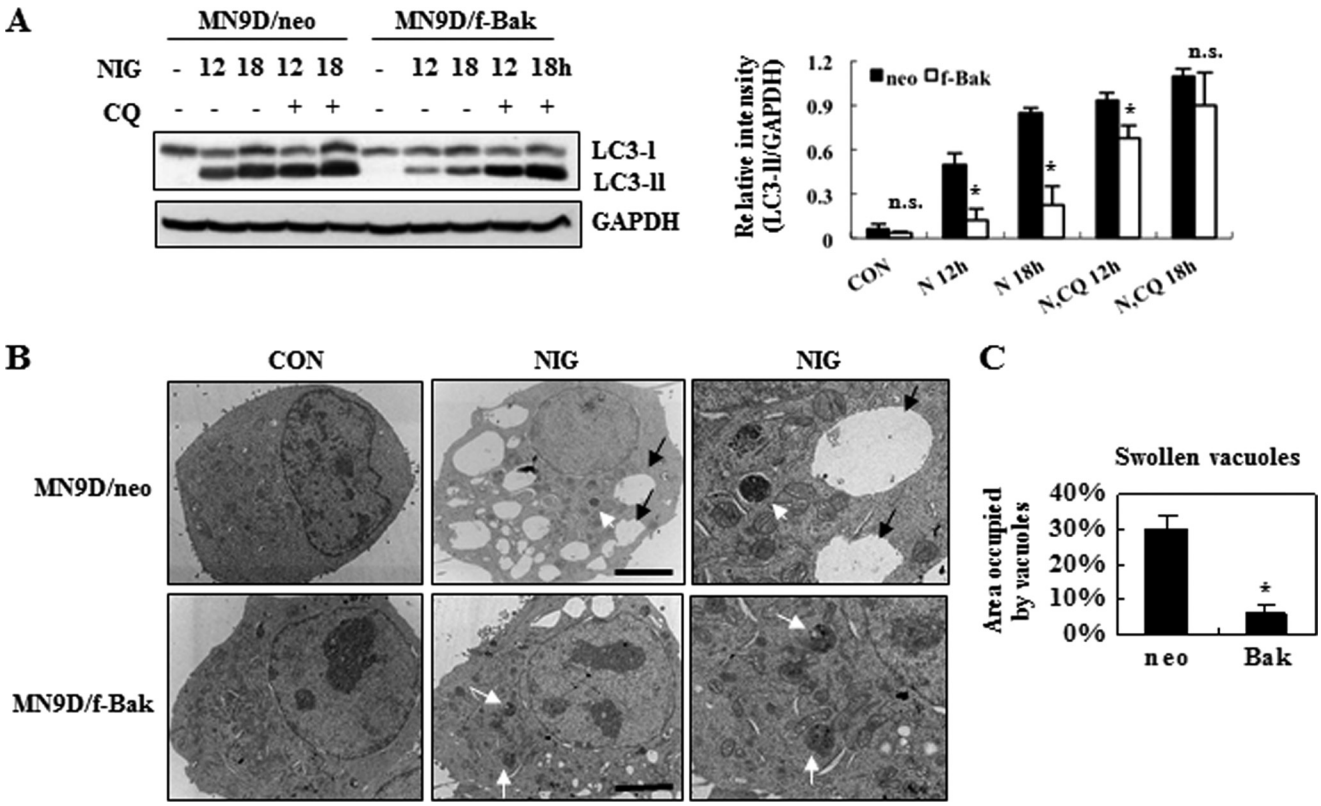

FIGURE 8. **Bak attenuates nigericin-induced cell death by maintaining autophagic flux.** *A*, MN9D cells stably overexpressing empty vector (MN9D/neo) or FLAG-tagged Bak (MN9D/f-Bak) were treated with 0.1 μM nigericin in the presence or the absence of 10 μM CQ for the indicated time periods. Cell lysates were separated, transblotted, and probed with anti-LC3 and -GAPDH antibodies. Quantitation of the relative intensity of LC3-II normalized to GAPDH was carried out. Each *bar* represents the mean ± S.D. (*error bars*) from three independent experiments. *B*, ultrastructural photomicrographs of MN9D/neo and MN9D/f-Bak cells treated with or without 0.1 μM nigericin for 9 h. *Scale bar*, 5 μm. Autophagic vacuoles and swollen vacuoles in nigericin-treated cells were indicated by *white arrows* and by *black arrows*, respectively. *Enlarged images* of the same microscopic field in nigericin-treated MN9D/neo and MN9D/f-Bak cells are shown at the *right*. *C*, the area occupied by abnormally swollen vacuoles following nigericin treatment was measured with Scion Image. Values were shown as a percentage of the area occupied by swollen vacuoles over the total area of the cell. Thirty cells from two independent experiments were measured. *, $p < 0.05$; *n.s.*, not significant.

mulation and swollen vacuole formation following nigericin treatment, it would be very intriguing to investigate how the BH3 domain distinctively plays a role in both apoptosis and autophagy. The BH3 domain of Bak or Bax has been demonstrated to be required for interaction with Bcl-2 family proteins or BH3-only proteins (17). Based on previous studies by others demonstrating that members of the Bcl-2 family actively influence autophagic events by regulating the rate of interaction with Beclin 1, another BH3-only protein (21–24, 44), it may be likely that mapping the interactions with Bcl-2 family members or finding novel binding profiles of Bak may be the key to understanding the mechanisms by which Bak regulates nigericin-induced autophagic cell death. The implication of Ca^{2+} in autophagy has been also investigated (45). Our unpublished data[3] indicated that the nigericin-induced increased level of intracellular free Ca^{2+} is significantly attenuated in MN9D cells overexpressing Bak. Similarly, we observed that dysregulation of cytosolic Ca^{2+} can impair autophagic flux in MN9D cells. Under these conditions, therefore, we found that the chelation of cytosolic Ca^{2+} or overexpression of calcium-binding protein enhances autophagic flux during nigericin-induced neurodegeneration.[3] Considering that a large amount of Bak is expressed in the mitochondria of MN9D cells, we are tempted to propose that the mitochondrially localized Bak seems to block drug-induced increased cytosolic Ca^{2+} level and consequently actively regulate autophagic flux. Because a common characteristic of neurodegenerative disorders is typically the accumulation of protein aggregates, it would be very intriguing to investigate whether Bak also plays a critical role in maintenance of protein homeostasis in experimental models of Alzheimer, Parkinson, and Huntington disease. Through direct examination of how Bak is involved in regulating these events and perhaps expansion of recent evidence of Bax regulatory activity on autophagy (46, 47), for example, we would be able to gain a better understanding of the function of the Bcl-2 family proteins in the regulation of autophagy and of its potential as a novel therapeutic strategy in neurodegeneration.

Acknowledgments—We thank Dr. Yoshimory (Osaka University) and Dr. Reed (Burnham Institute) for the generous gifts of GFP-tagged LC3 and human Bak cDNA, respectively. We thank Dr. Jürgen Roth (University of Zurich) for assistance in analyzing the electron micrographs in general and swollen vacuoles in particular.

REFERENCES

1. Kroemer, G., Mariño, G., and Levine, B. (2010) Autophagy and the integrated stress response. *Mol. Cell* **40,** 280–293
2. He, C., and Klionsky, D. J. (2009) Regulation mechanisms and signaling

pathways of autophagy. *Annu. Rev. Genet.* **43,** 67–93
3. Kabeya, Y., Mizushima, N., Ueno, T., Yamamoto, A., Kirisako, T., Noda, T., Kominami, E., Ohsumi, Y., and Yoshimori, T. (2000) LC3, a mammalian homologue of yeast Apg8p, is localized in autophagosome membranes after processing. *EMBO J.* **19,** 5720–5728
4. Tanida, I., Minematsu-Ikeguchi, N., Ueno, T., and Kominami, E. (2005) Lysosomal turnover, but not a cellular level, of endogenous LC3 is a marker for autophagy. *Autophagy* **1,** 84–91
5. Eskelinen, E. L. (2005) Maturation of autophagic vacuoles in mammalian cells. *Autophagy* **1,** 1–10
6. Fader, C. M., and Colombo, M. I. (2009) Autophagy and multivesicular bodies. Two closely related partners. *Cell Death Differ.* **16,** 70–78
7. Filimonenko, M., Stuffers, S., Raiborg, C., Yamamoto, A., Malerød, L., Fisher, E. M., Isaacs, A., Brech, A., Stenmark, H., and Simonsen, A. (2007) Functional multivesicular bodies are required for autophagic clearance of protein aggregates associated with neurodegenerative disease. *J. Cell Biol.* **179,** 485–500
8. Jäger, S., Bucci, C., Tanida, I., Ueno, T., Kominami, E., Saftig, P., and Eskelinen, E. L. (2004) Role for Rab7 in maturation of late autophagic vacuoles. *J. Cell Sci.* **117,** 4837–4848
9. Lee, J. A., Beigneux, A., Ahmad, S. T., Young, S. G., and Gao, F. B. (2007) ESCRT-III dysfunction causes autophagosome accumulation and neurodegeneration. *Curr. Biol.* **17,** 1561–1567
10. Galluzzi, L., Aaronson, S. A., Abrams, J., Alnemri, E. S., Andrews, D. W., Baehrecke, E. H., Bazan, N. G., Blagosklonny, M. V., Blomgren, K., Borner, C., Bredesen, D. E., Brenner, C., Castedo, M., Cidlowski, J. A., Ciechanover, A., Cohen, G. M., De Laurenzi, V., De Maria, R., Deshmukh, M., Dynlacht, B. D., El-Deiry, W. S., Flavell, R. A., Fulda, S., Garrido, C., Golstein, P., Gougeon, M. L., Green, D. R., Gronemeyer, H., Hajnóczky, G., Hardwick, J. M., Hengartner, M. O., Ichijo, H., Jäättelä, M., Kepp, O., Kimchi, A., Klionsky, D. J., Knight, R. A., Kornbluth, S., Kumar, S., Levine, B., Lipton, S. A., Lugli, E., Madeo, F., Malomi, W., Marine, J. C., Martin, S. J., Medema, J. P., Mehlen, P., Melino, G., Moll, U. M., Morselli, E., Nagata, S., Nicholson, D. W., Nicotera, P., Nunez, G., Oren, M., Penninger, J., Pervaiz, S., Peter, M. E., Piacentini, M., Prehn, J. H., Puthalakath, H., Rabinovich, G. A., Rizzuto, R., Rodrigues, C. M., Rubinsztein, D. C., Rudel, T., Scorrano, L., Simon, H. U., Steller, H., Tschopp, J., Tsujimoto, Y., Vandenabeele, P., Vitale, I., Vousden, K. H., Youle, R. J., Yuan, J., Zhivotovsky, B., and Kroemer, G. (2009) Guidelines for the use and interpretation of assays for monitoring cell death in higher eukaryotes. *Cell Death Differ.* **16,** 1093–1107
11. Scarlatti, F., Granata, R., Meijer, A. J., and Codogno, P. (2009) Does autophagy have a license to kill mammalian cells? *Cell Death Differ.* **16,** 12–20
12. Kroemer, G., and Levine, B. (2008) Autophagic cell death. The story of a misnomer. *Nat. Rev. Mol. Cell Biol.* **9,** 1004–1010
13. Eisenberg-Lerner, A., Bialik, S., Simon, H. U., and Kimchi, A. (2009) Life and death partners. Apoptosis, autophagy, and the cross-talk between them. *Cell Death Differ.* **16,** 966–975
14. Kroemer, G., Galluzzi, L., Vandenabeele, P., Abrams, J., Alnemri, E. S., Baehrecke, E. H., Blagosklonny, M. V., El-Deiry, W. S., Golstein, P., Green, D. R., Hengartner, M., Knight, R. A., Kumar, S., Lipton, S. A., Malorni, W., Nuñez, G., Peter, M. E., Tschopp, J., Yuan, J., Piacentini, M., Zhivotovsky, B., Melino, G., and the Nomenclature Committee on Cell Death 2009 (2009) Classification of cell death. Recommendations of the Nomenclature Committee on Cell Death 2009. *Cell Death Differ.* **16,** 3–11
15. Maiuri, M. C., Zalckvar, E., Kimchi, A., and Kroemer, G. (2007) Self-eating and self-killing. Cross-talk between autophagy and apoptosis. *Nat. Rev. Mol. Cell Biol.* **8,** 741–752
16. Gross, A., McDonnell, J. M., and Korsmeyer, S. J. (1999) BCL-2 family members and the mitochondria in apoptosis. *Genes Dev.* **13,** 1899–1911
17. Chipuk, J. E., Moldoveanu, T., Llambi, F., Parsons, M. J., and Green, D. R. (2010) The BCL-2 family reunion. *Mol. Cell* **37,** 299–310
18. Kim, H., Tu, H. C., Ren, D., Takeuchi, O., Jeffers, J. R., Zambetti, G. P., Hsieh, J. J., and Cheng, E. H. (2009) Stepwise activation of BAX and BAK by tBID, BIM, and PUMA initiates mitochondrial apoptosis. *Mol. Cell* **36,** 487–499
19. Liang, X. H., Kleeman, L. K., Jiang, H. H., Gordon, G., Goldman, J. E., Berry, G., Herman, B., and Levine, B. (1998) Protection against fatal Sindbis virus encephalitis by Beclin, a novel Bcl-2-interacting protein. *J. Virol.* **72,** 8586–8596
20. Maiuri, M. C., Le Toumelin, G., Criollo, A., Rain, J. C., Gautier, F., Juin, P., Tasdemir, E., Pierron, G., Troulinaki, K., Tavernarakis, N., Hickman, J. A., Geneste, O., and Kroemer, G. (2007) Functional and physical interaction between Bcl-X_L and a BH3-like domain in Beclin-1. *EMBO J.* **26,** 2527–2539
21. Høyer-Hansen, M., Bastholm, L., Szyniarowski, P., Campanella, M., Szabadkai, G., Farkas, T., Bianchi, K., Fehrenbacher, N., Elling, F., Rizzuto, R., Mathiasen, I. S., and Jäättelä, M. (2007) Control of macroautophagy by calcium, calmodulin-dependent kinase kinase-β, and Bcl-2. *Mol. Cell* **25,** 193–205
22. Strappazzon, F., Vietri-Rudan, M., Campello, S., Nazio, F., Florenzano, F., Fimia, G. M., Piacentini, M., Levine, B., and Cecconi, F. (2011) Mitochondrial BCL-2 inhibits AMBRA1-induced autophagy. *EMBO J.* **30,** 1195–1208
23. Erlich, S., Mizrachy, L., Segev, O., Lindenboim, L., Zmira, O., Adi-Harel, S., Hirsch, J. A., Stein, R., and Pinkas-Kramarski, R. (2007) Differential interactions between Beclin 1 and Bcl-2 family members. *Autophagy* **3,** 561–568
24. Malik, S. A., Orhon, I., Morselli, E., Criollo, A., Shen, S., Marino, G., Benyounes, A., Benit, P., Rustin, P., Maiuri, M. C., and Kroemer, G. (2011) BH3 mimetics activate multiple pro-autophagic pathways. *Oncogene* **30,** 3918–3929
25. Steinrauf, L. K., Czerwinski, E. W., and Pinkerton, M. (1971) Comparison of the monovalent cation complexes of monensin, nigericin, and dianemycin. *Biochem. Biophys. Res. Commun.* **45,** 1279–1283
26. Zhang, L., Yu, J., Pan, H., Hu, P., Hao, Y., Cai, W., Zhu, H., Yu, A. D., Xie, X., Ma, D., and Yuan, J. (2007) Small molecule regulators of autophagy identified by an image-based high-throughput screen. *Proc. Natl. Acad. Sci. U.S.A.* **104,** 19023–19028
27. Grinde, B. (1983) Effect of carboxylic ionophores on lysosomal protein degradation in rat hepatocytes. *Exp. Cell Res.* **149,** 27–35
28. Kawai, A., Uchiyama, H., Takano, S., Nakamura, N., and Ohkuma, S. (2007) Autophagosome-lysosome fusion depends on the pH in acidic compartments in CHO cells. *Autophagy* **3,** 154–157
29. Oh, J. H., O'Malley, K. L., Krajewski, S., Reed, J. C., and Oh, Y. J. (1997) Bax accelerates staurosporine-induced but suppresses nigericin-induced neuronal cell death. *Neuroreport* **8,** 1851–1856
30. Kim, J. E., Oh, J. H., Choi, W. S., Chang, I. I., Sohn, S., Krajewski, S., Reed, J. C., O'Malley, K. L., and Oh, Y. J. (1999) Sequential cleavage of poly(ADP-ribose)polymerase and appearance of a small Bax-immunoreactive protein are blocked by Bcl-X_L and caspase inhibitors during staurosporine-induced dopaminergic neuronal apoptosis. *J. Neurochem.* **72,** 2456–2463
31. Lee, Y. M., Park, S. H., Shin, D. I., Hwang, J. Y., Park, B., Park, Y. J., Lee, T. H., Chae, H. Z., Jin, B. K., Oh, T. H., and Oh, Y. J. (2008) Oxidative modification of peroxiredoxin is associated with drug-induced apoptotic signaling in experimental models of Parkinson disease. *J. Biol. Chem.* **283,** 9986–9998
32. Lim, J., Kim, H. W., Youdim, M. B., Rhyu, I. J., Choe, K. M., and Oh, Y. J. (2011) Binding preference of p62 toward LC3-II during dopaminergic neurotoxin-induced impairment of autophagic flux. *Autophagy* **7,** 51–60
33. Hansen, M. B., Nielsen, S. E., and Berg, K. (1989) Re-examination and further development of a precise and rapid dye method for measuring cell growth/cell kill. *J. Immunol. Methods* **119,** 203–210
34. Ylä-Anttila, P., Vihinen, H., Jokitalo, E., and Eskelinen, E. L. (2009) Monitoring autophagy by electron microscopy in mammalian cells. *Methods Enzymol.* **452,** 143–164
35. Thorens, B., and Roth, J. (1996) Intracellular targeting of GLUT4 in transfected insulinoma cells. Evidence for association with constitutively recycling vesicles distinct from synaptophysin and insulin vesicles. *J. Cell Sci.* **109,** 1311–1323
36. Iwai-Kanai, E., Yuan, H., Huang, C., Sayen, M. R., Perry-Garza, C. N., Kim, L., and Gottlieb, R. A. (2008) A method to measure cardiac autophagic flux *in vivo*. *Autophagy* **4,** 322–329
37. Komatsu, M., Waguri, S., Koike, M., Sou, Y. S., Ueno, T., Hara, T., Mizushima, N., Iwata, J., Ezaki, J., Murata, S., Hamazaki, J., Nishito, Y., Iemura,

S., Natsume, T., Yanagawa, T., Uwayama, J., Warabi, E., Yoshida, H., Ishii, T., Kobayashi, A., Yamamoto, M., Yue, Z., Uchiyama, Y., Kominami, E., and Tanaka, K. (2007) Homeostatic levels of p62 control cytoplasmic inclusion body formation in autophagy-deficient mice. *Cell* **131,** 1149–1163
38. Pinkerton, M., and Steinrauf, L. K. (1970) Molecular structure of monovalent metal cation complexes of monensin. *J. Mol. Biol.* **49,** 533–546
39. Boya, P., González-Polo, R. A., Casares, N., Perfettini, J. L., Dessen, P., Larochette, N., Métivier, D., Meley, D., Souquere, S., Yoshimori, T., Pierron, G., Codogno, P., and Kroemer, G. (2005) Inhibition of macroautophagy triggers apoptosis. *Mol. Cell Biol.* **25,** 1025–1040
40. Wong, E., and Cuervo, A. M. (2010) Autophagy gone awry in neurodegenerative diseases. *Nat. Neurosci.* **13,** 805–811
41. Cook, N. R., Row, P. E., and Davidson, H. W. (2004) Lysosome-associated membrane protein 1 (Lamp1) traffics directly from the TGN to early endosomes. *Traffic* **5,** 685–699
42. Luzio, J. P., Poupon, V., Lindsay, M. R., Mullock, B. M., Piper, R. C., and Pryor, P. R. (2003) Membrane dynamics and the biogenesis of lysosomes. *Mol. Membr. Biol.* **20,** 141–154
43. Tait, S. W., and Green, D. R. (2010) Mitochondria and cell death. Outer membrane permeabilization and beyond. *Nat. Rev. Mol. Cell Biol.* **11,** 621–632
44. Maiuri, M. C., Criollo, A., Tasdemir, E., Vicencio, J. M., Tajeddine, N., Hickman, J. A., Geneste, O., and Kroemer, G. (2007) BH3-only proteins and BH3 mimetics induce autophagy by competitively disrupting the interaction between Beclin 1 and Bcl-2/Bcl-X_L. *Autophagy* **3,** 374–376
45. Høyer-Hansen, M., and Jäättelä, M. (2007) Connecting endoplasmic reticulum stress to autophagy by unfolded protein response and calcium. *Cell Death Differ.* **14,** 1576–1582
46. Yee, K. S., Wilkinson, S., James, J., Ryan, K. M., and Vousden, K. H. (2009) PUMA- and Bax-induced autophagy contributes to apoptosis. *Cell Death Differ.* **16,** 1135–1145
47. Luo, S., and Rubinsztein, D. C. (2010) Apoptosis blocks Beclin 1-dependent autophagosome synthesis. An effect rescued by Bcl-xL. *Cell Death Differ.* **17,** 268–277